

An improved snowfall monitoring system developed in central Niigata Prefecture, Japan

Katsuya YAMASHITA^{1*}, Sento NAKAI¹, Hiroki MOTOYOSHI¹ and Masaaki ISHIZAKA¹

¹ Snow and Ice Research Center, National Research Institute for Earth Science and Disaster Resilience, Suyoshi, Nagaoka, Niigata, 940-0821 Japan

* yamashita@bosai.go.jp

(Received September 19, 2017; Revised manuscript accepted January 25, 2019)

Abstract

Meteorological radars are important for quantitative precipitation estimation (QPE) as they can determine precipitation distribution with high spatiotemporal resolution. However, accurate QPE of solid precipitation remains challenging despite its importance. A precise QPE algorithm requires an appropriate radar reflectivity-precipitation rate (Ze-R) relationship corresponding to the precipitation type, assessment of the change in size and fall velocity of snow particles falling below the radar beam, and validation using accurate precipitation amounts at the surface. In order to address these requirements, the study established an improved snowfall monitoring system, named the Concentrated Snowfall Monitoring System (CSMS) in central Niigata Prefecture. The CSMS was composed of an X-band radar and six ground observation sites. Optical disdrometers were installed at all sites to classify the precipitation type and select the appropriate Ze-R relationship. Vertical profiles of the precipitation particles and thermodynamic environment below the radar beam were assessed using micro rain radars and microwave radiometers. Presently, the precipitation amounts measured using tipping-bucket gauges are underestimated due to wind induced and wetting losses. Therefore, high accuracy weighing gauges were installed at three sites to quantify the underestimation. The CSMS data was used to conduct a preliminary analysis of the heavy snowfall that occurred on January 24 and 25, 2016, in central Niigata Prefecture. The designed CSMS estimated the precipitation distribution and precipitation type successfully. The results indicate that the CSMS can potentially determine an appropriate Ze-R relationship, which can improve the estimation of precipitation rates and contribute to the improved QPE of solid precipitation.

Key words: snow-related disaster, weather radar, ground observation, precipitation particle, QPE

1. Introduction

Heavy snowfall-related disasters have occurred frequently in Japan in recent years (Sato, 2006; Maeda, 2007; Sato, 2012; Nakai and Yamaguchi, 2012; Araki and Murakami, 2015; Yamazaki *et al.*, 2015; Honda *et al.*, 2016). Although accurate forecasts of heavy snowfall using numerical weather models can reduce the damage caused by snowfall-related disasters, obtaining such forecasts is currently difficult. An effective solution can be derived using a combination of real-time observations and numerical weather forecast data.

Weather radars can effectively measure the characteristics of the mesoscale cloud system, which cause severe weather (Wakimoto and Srivastava, 2003; Doviak and Zrinc, 1993; Fabry, 2015). However, the accuracy of quantitative precipitation estimation (QPE) for solid precipitation is unsatisfactory given the highly diverse relationship between the radar reflectivity factor (Ze) and precipitation rate (R), and the effect of multiple parameters, such as crystal type, degree of riming and

aggregation, density, and terminal velocity (Fujiyoshi *et al.*, 1990; Rasmussen *et al.*, 2003; Zhang, 2016).

Therefore, a QPE algorithm that identifies an appropriate Ze-R relationship and acknowledges particle size and phase changes below the radar beam level needs to be developed. Further, a technique to classify precipitation type in real-time is needed.

The Japan Meteorological Agency established the Automated Meteorological Data Acquisition System (AMeDAS), which collects regional weather data using a surface weather observation network. In the AMeDAS, precipitation is measured using a tipping-bucket gauge. However, a non-negligible catch loss due to wind induced and wetting losses is encountered during solid precipitation measurements (Goodison *et al.*, 1998; Yokoyama *et al.*, 2003). Therefore, a method to correct the precipitation amount should be developed in the QPE algorithm.

The study developed and tested a new observation system to address these issues. The observation system was constructed in the central part of Niigata Prefecture, which is designated as a heavy snowfall region by the Japanese government. The system was composed of an

X-band polarimetric Doppler radar and multiple ground observation sites. The ground observation sites obtained precipitation rate and precipitation type on the ground within the observation range of the weather radar; the radar acquired the distribution of precipitation with higher spatial resolution compared to ground observation. The ground observation sites also obtained vertical profiles of the precipitation particles and thermodynamic environment to investigate cloud microphysical processes affecting size and fall velocity of precipitation particles. The study proposed that the precipitation rate estimations of the weather radar will improve when a combination of measured weather radar values and ground observation data is used. Weighing precipitation gauges surrounded by Double Fence Intercomparison Reference (DFIR: see Rasmussen *et al.*, 2012) wind shields were installed at two ground observation sites to accurately measure the precipitation amounts. Equations to correct the catch loss of the tipping-bucket were derived by analyzing the difference in precipitation amounts between the weighing gauge in the DFIR and operational tipping-bucket gauges. Ground-based data collected by the AMeDAS was used to verify the QPE accuracy using the CSMS data. The overview of the observation system, methods to determine the predominant precipitation type, and preliminary results are described in Sections 2, 3, and 4, respectively. Section 5 summarizes the paper. Japan Standard Time (JST) was used in this paper.

2. The Concentrated Snowfall Monitoring System (CSMS) –an improved snowfall monitoring system

The observation range of the X-band polarimetric Doppler radar was 80 km from the Snow and Ice Research Center (SIRC) in Nagaoka city. All six ground observation sites were located within the observation range of the radar (Fig. 1). The ground observation sites provided the following data: (1) predominant precipitation type with high temporal resolution at multiple points to identify the Ze-R relationship, which was used for the radar QPE, (2) shapes of the precipitation particles, which was used to confirm whether the classification of predominant precipitation type using particle size and fall velocity is reasonable or not, (3) ground snowfall data, (4) catch loss of snow of tipping-buckets used by the AMeDAS, (5) vertical profile of precipitation particles from the lowest radar observable level to the ground, and (6) motion and structure of precipitating clouds.

The ground observation sites, referred to as the Snow Particle observation Line (SPLine), are comprised of three full-specification sites (F-sites) and three simple specification sites (S-sites). The F-sites were located at the SIRC (S in Fig. 1) in Nagaoka city, Niigata Institute of Technology in Kashiwazaki city (K in Fig. 1), and Hokuriku National Agricultural Experiment Station of the National Agriculture and Food Research Organization in

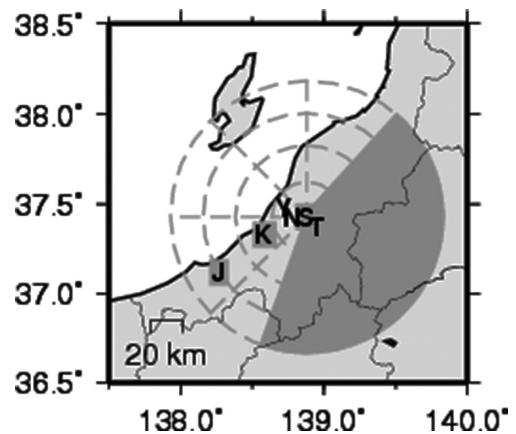


Fig. 1. Location of the Snow Particle observation Line (SPLine) sites. S, K, J, N, T, and Y, respectively, indicate sites at the SIRC, Kashiwazaki, Joetsu, Nagaoka University of Technology, Tochio-Tashiro, and Nishiyama-Yakushi. The dashed circles indicate concentric circles spaced at 20km intervals centered on MP2. The dashed radial lines indicate azimuth every 45 degrees. The area indicated by the shadow on the southeast side of the SIRC is the area where the radar beam was blocked by mountains.

Joetsu city (J in Fig. 1). The F-sites were arranged along the direction of the snowbands of vortex disturbances, which often contribute to heavy snowfall. The S-sites were located at Nagaoka University of Technology (N in Fig. 1) in Nagaoka city, Tochio-Tashiro (T in Fig. 1) in Nagaoka city, and Nishiyama-Yakushi (Y in Fig. 1) in Kashiwazaki city. The S-sites were arranged along the direction of long-lasting cloud streets, which also contribute to heavy snowfall. The CSMS offered multiple advantages, including adjustment of the installation height of the instruments, installation of appropriate heaters, and installation of wind shields to facilitate data collection, even during heavy snowfall.

Tables 1 and 2 indicate the specifications of instruments utilized and locations of the ground observation sites, respectively. At the F-sites, a two-dimensional video disdrometer (2DVD) and an optical disdrometer laser precipitation monitor (LPM) were installed to measure the characteristics of the precipitation particles on the ground. Specifically, 2DVD was employed to capture the shape of precipitation particles from two directions. Precipitation amount was measured using several sensors, namely, weighing gauge (Geonor with Alter shield), a Tamura snow rain intensity meter (Tamura) for comparison with other observations conducted at the SIRC, and tipping-bucket gauges for comparison with operational AMeDAS measurements. Air pressure, temperature, wind speed, wind direction, and relative humidity were also measured at the F-sites. In addition, a microwave radiometer (MWR) was used to estimate the vertical profiles of temperature, liquid water content (LWC), and water vapor using incoming microwave radiation, and a micro rain radar (MRR) was used to estimate the vertical profiles of reflectivity and

Table 1. Specifications of instruments utilized for the CSMS.

Instrument Name	Manufacturer	Model	Measurement parameter	Sampling time	Reference
Windmill type anemometer (Windmill)	Young. Co.	05103	WD, WS	1 min	http://www.youngusa.com/
Ventilated thermohygrometer (VTH)	Vaisala com.	HMP155D	T, RH	1 min	http://www.vaisala.com/
Compact weather station (CWS)	G. Lufft Mess- und Regeltechnik GmbH	WS600-UMB	T,P,RH,WD,WS	1min	http://www.lufft.com/en/
Hot water type tipping bucket gauge (RT-3)	Ogasawara Keiki Co.	RS-222A	PI	1min	Goodison <i>et al.</i> (1998)
Spill type tipping bucket gauge (RT-4)	Yokogawa Denshikiki Co.	B-071	PI	1min	Goodison <i>et al.</i> (1998)
Geonor weighing gauge (Geonor)	Geonor Inc.	T-200B-MD3W	PI	1min	Bakkehoi <i>et al.</i> (1985)
Tamura snow-rain intensity meter (Tamura)	Sanyo Industry Co.	SR-2-N	PI	1min	Tamura (1993)
Laser Precipitation Monitor (LPM)	Adolf Thies GmbH & Co. KG	5.4110.01.000	PI, DSD, V	1min	Bloemink and Lanzinger (2005)
2D Video Disdrometer (2DVD)	Joanneum Research		PI, DSD, V, Oblateness, Particle Image	>18 micro sec	Kruger and Krajewski (2002)
Micro Rain Radar (MRR)	METEK Co.	MRR-2	Profile of Ze, Vd	>10 sec	Maahn and Kollias (2012)
MicroWave Radiometer (MWR)	Radiometrics Co.	MP-3000A	Profile of T, RH, WV, and LWC	>10 sec	Solheim <i>et al.</i> (1998)

*WD:Wind Drection, WS:Wind Speed, T:Temperature, P:Pressure, RH: Relative Humidity, PI: Precipitation Intensity, DSD: Drop Size Distribution, V: falling Velocity, Ze: Reflectivity factor, Vd: Doppler velocity, WV: Water Vapor, LWC: Liquid Water Content

Table 2. Location and instruments of the SPLine ground observation sites.

Site	SIRC (Nagaoka)	Kashiwazaki	Joetsu	Nagaoka University of Technology (Nagaoka)	Tochio-Tashiro (Nagaoka)	Nishiyama-Yakushi (Kashiwazaki)
Longitude (°E)	138.88	138.58	138.27	138.78	138.95	138.72
Latitude (°N)	37.43	37.33	37.12	37.43	37.37	37.48
Altitude (m)	97	15	10	55	420	320
WS-Windmill	○	○	○	—	○	○
WD-Windmill	○	○	○	—	○	○
WS-CWS	○	○	○	○	—	—
WD-CWS	○	○	○	○	—	—
T-VTH	○	○	○	—	○	○
RH-VTH	○	○	○	—	○	○
T-CWS	○	○	○	○	—	—
RH-CWS	○	○	○	○	—	—
RT-3	○	○	○	—	○	○
RT-4	○	○	○	—	—	—
Geonor	○	○	○	—	—	—
Tamura	○	○	○	○	○	○
LPM	○	○	○	○	○	○
2DVD	○	○	○	—	—	—
MRR	○	○	○	—	—	—
MWR	○	○	○	—	—	—

*WD:Wind Drection, WS:Wind Speed, T:Temperature, P:Pressure, RH: Relative Humidity, PI: Precipitation Intensity, DSD: Drop Size Distribution, V: falling Velocity, Ze: Reflectivity factor, Vd: Doppler velocity, WV: Water Vapor, LWC: Liquid Water Content

Doppler velocity of precipitation particles from vertically radiated K-band electromagnetic waves at the F-sites. At the S-sites, LPMs, Tamura meters, compact weather stations, and tipping-bucket gauges were installed to facilitate precipitation particle observations. Two types of tipping-bucket gauges adopted by the AMeDAS, namely Model RT-3 and Model RT-4, were used to measure precipitation rate in the SPLine. Model RT-3 (Ogasawara Keiki Co.) had a thick wall filled with hot water and did not have a wind shield. Model RT-4 (Yokogawa Denshikiki Co.) accumulated precipitation in a reservoir with water heated to 5°C and had a cylindrical wind shield. Details of the tipping-bucket gauges are described in Annex 3F of Goodison *et al.* (1998).

An X-band polarimetric radar system for solid and wet precipitation observation (Multi-Phase Precipitation radar; MP2) was developed to determine the spatial distribution of snowfall. It was installed on the roof of the SIRC building and mainly observed a southwestern

semicircular area within an 80 km radius of the SIRC (Fig. 2). The specification of MP2 is summarized in Table 3.

Figure 3 presents the conceptual diagram of the data generated by the CSMS. A QPE method that utilized precipitation type was developed using the horizontal distribution of Ze from MP2 and precipitation type from the SPLine. Precipitation type was classified on the basis of the size and fall velocity data from the disdrometer. Further, the precipitation rate was calculated using the Ze-R relationship determined from precipitation types, such as snow aggregate and graupel. Thus, radar-disdrometer simultaneous observation was an important feature of the CSMS.

A major factor in the underestimation of solid precipitation obtained from operational tipping-bucket gauges is wind induced undercatch (Goodison *et al.*, 1998; Yokoyama *et al.*, 2003). Precipitation amounts from tipping-bucket gauges require correction during QPE validation. At the Joetsu and SIRC sites, Geonors were installed in the

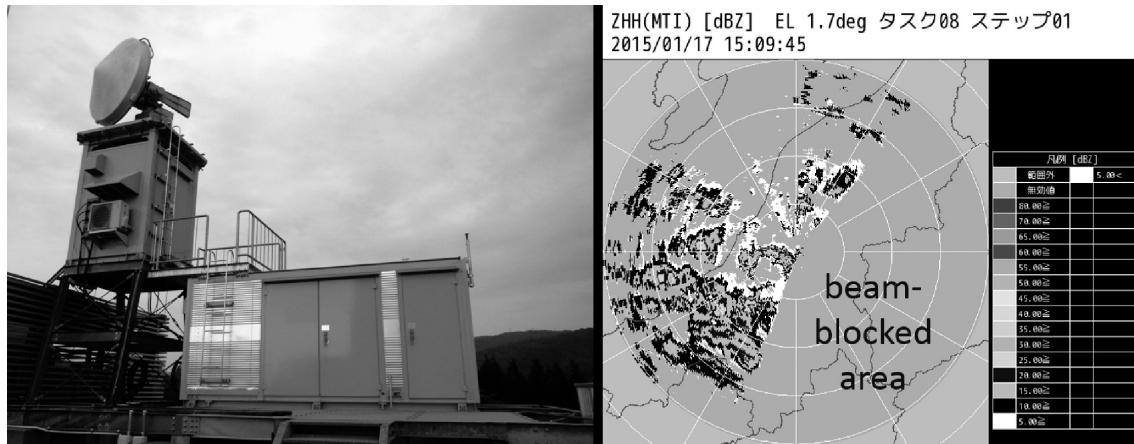


Fig. 2. Photograph and sample image of MP2. The observation range was within 80 km.

Table 3. Specifications of MP2 at the SIRC.

Radar	MP2
Antenna diameter	2.2 m
Beamwidth	$<1.2^\circ$
Gain	45 dB
Polarization	H, V, H+V
Transmitter	Solid-state transmitter
Transmitting peak power	200 W (H) + 200 W (V)
Transmitting frequency	9445 MHz
Pulse length	1.0 μ s, 32 μ s
Maximum pulse repetition frequency	1500 Hz
Minimum detectable signal	-110 dBm
Observation range	80 km

Note: H and V indicate horizontal and vertical polarization, respectively.

DFIR to accurately measure the precipitation amount. Equations to correct the catch loss of the tipping-bucket gauges were derived by analyzing the difference in precipitation amounts between the Geonors in the DFIR and the operational tipping-bucket gauges.

Scanning weather radars cannot observe near the ground at large distances because of ground clutter, beam blockage by topography, and curvature of the Earth's surface. For example, when the lowest available elevation angle is 1.7 degrees at a distance of 40 km, the corresponding lowest observed altitude is 1.2 km. Hence, change in the physical properties of precipitation particles (such as size, fall velocity, and Ze-R relationship) from the lowest radar observable level to the ground should be accounted for. Therefore, MRRs and MWRs were installed at the F-sites to observe these changes. The MRRs detected vertical changes in precipitation parameters (such as reflectivity factor and Doppler velocity) at low altitudes (below 1500 m), which cannot be easily detected by scanning weather radars, such as MP2. The MWR monitored the thermodynamic environment affecting vertical changes in the precipitation particles.

3. Method to determine the predominant precipitation type using particle size and fall velocity

We adapted the methodology described in Ishizaka *et al.* (2013, 2016) to determine the predominant precipitation type using particle size and fall velocity, which were measured by optical disdrometers of the CSMS. Ishizaka *et al.* (2013) proposed a method for objectively identifying the type of precipitation contributing to snowfall during any arbitrary period using the Center of Mass Flux (CMF), which is defined as the mass-flux weighted mean value of particle size and fall velocity. This method enables quantitative identification of the main precipitation types based on the locations of CMFs in the size and velocity coordinate system (Fig. 4). The empirical curves of various precipitation types described by Ishizaka *et al.* (2016) were used as classification boundaries with the exception of the rain group. Rain, graupel, aggregate, small particle category 1 (S1), and small particle category 2 (S2) were classified on the basis of the boundary highlighted in Fig. 4. The rain group was defined as the CMF located within 20% of the empirical curve for rain (Atlas and Ulbrich, 1977). The region where the fall velocity range was between the boundary of the rain group and the "graupel-like snow of lump type" empirical curve (Locatelli and Hobbs, 1974) was defined as the graupel group. The region that encompassed fall velocities slower than the lower boundary of the graupel groups and sizes larger than 4 mm was defined as the aggregate group. The remaining region in the size-fall velocity coordinates was classified as the small-particle category, which was divided into two regions (S1 and S2), and the boundary was the "graupel-like snow of hexagonal type" (Locatelli and Hobbs, 1974).

4. Preliminary observation results

Heavy snowfall occurred around the plains of central Niigata Prefecture on January 24 and January 25, 2016.

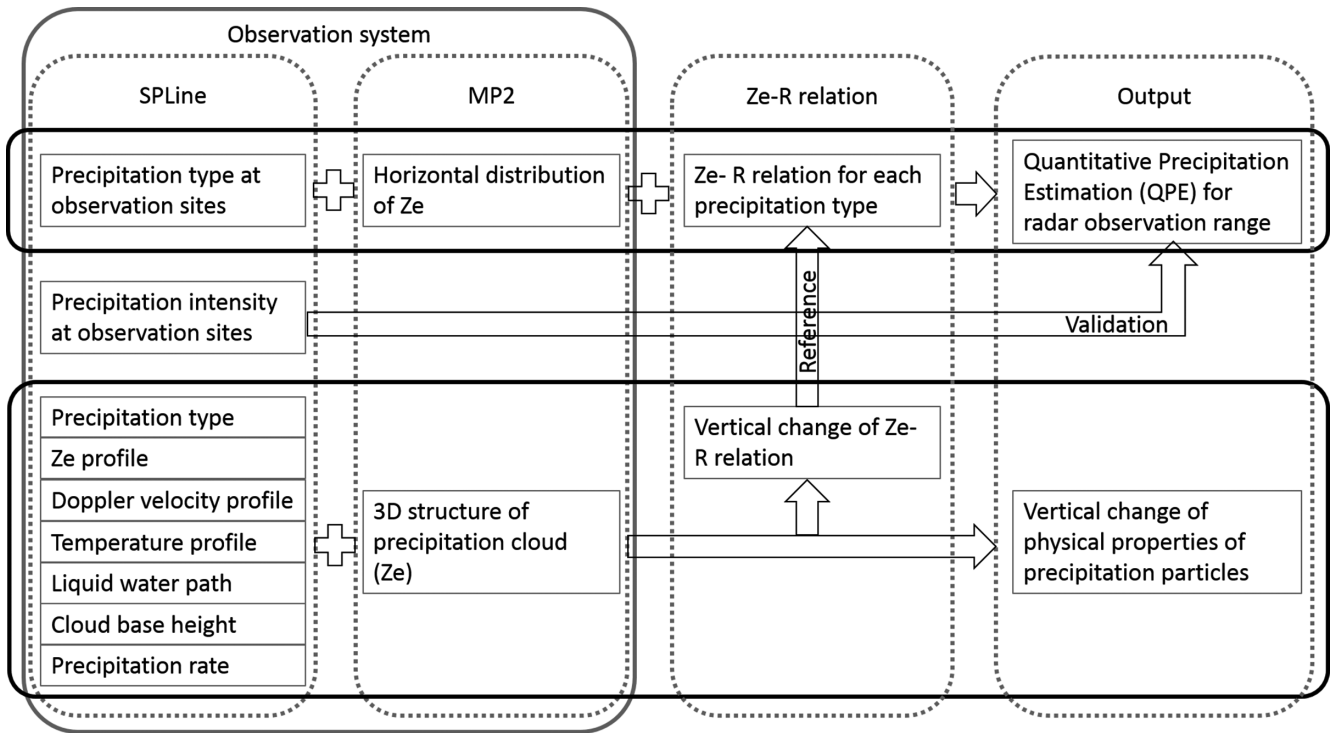


Fig. 3. Conceptual diagram generated by the CSMS.

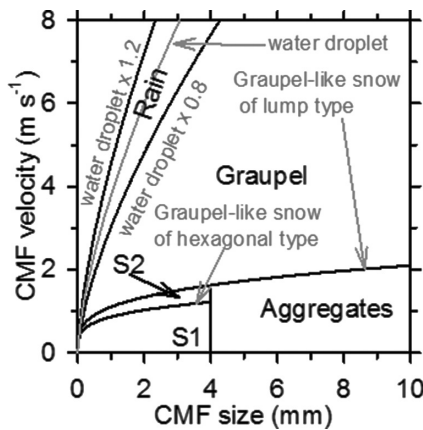


Fig. 4. Categories used in precipitation type classification modified from Ishizaka *et al.* (2016). The curves indicate the empirical curves of rain (Atlas and Ulbrich 1977), graupel-like snow of lump type (Locatelli and Hobbs 1974), graupel-like snow of hexagonal type (Locatelli and Hobbs 1974), and aggregates of unrimed assemblages of plates, side planes, bullets, and columns (Locatelli and Hobbs 1974).

Observations recorded during in this period (study period) were assessed to demonstrate the ability of the CSMS to generate data from the radar QPE, even during heavy snowfall. A time series of daily snowfall depths at the SIRC in January 2016 is depicted in Fig. 5. The snowfall depth between 09:00 JST on January 24 and 09:00 JST 25, 2016, was 83.2 cm, the fourth largest snowfall depth recorded at the SIRC since 1965. Train services were cancelled, the Hokuriku road expressway closed, and prolonged periods of traffic congestion on a

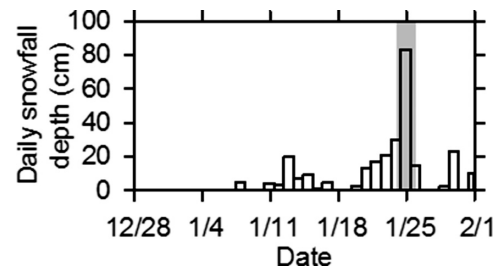


Fig. 5. Time series of daily snowfall depth in January 2016 at the SIRC, using the snow measurement board. The shaded area indicates a period of heavy snowfall from January 24 to 25, 2016. The snowfall depth is the depth of snowfall from 09:00 JST on the previous day until 09:00 JST on the indicated day.

major national road (Route 8) due to the heavy snow were reported, significantly affecting human activity in the plains of central Niigata Prefecture.

4.1 Distribution of solid precipitation

Figure 6 shows the time series of accumulated precipitation obtained at the SIRC and Joetsu sites during the study period. The accumulated precipitation measured by the Geonor placed in the DFIR (DFIR-Geonor) at the SIRC and Joetsu sites at 24:00 JST on January 25, 2016, was 128.4 and 33.2 mm, respectively. The accumulated precipitation of the tipping-bucket gauges (RT-3 and RT-4) was less than the DFIR-Geonor. Further, the differences were remarkable around 18:00 JST on January 24, 2016, at SIRC, and 08:00 JST on January 24, 2016, at Joetsu. The difference in the accumulated precipitation between DFIR-Geonor and

RT-4 at 24:00 JST on January 25, 2016, was about 16% at SIRC and 45% at Joetsu. This result indicated that the accumulated precipitation, obtained using the tipping-bucket gauges during the study period, was less than the actual amount. Therefore, a method to correct the catch loss was developed by analyzing the difference between the DFIR-Geonor and tipping-bucket gauges.

Figure 7 shows the distribution of accumulated precipitation during the study period, which was estimated from the reflectivity factor observed by MP2. Various Ze-R relationships were applied. Figure 7(a) illustrates the precipitation distribution using the Marshall-Palmer formula for stratiform rain (Marshall *et al.*, 1955) and snow (Marshall and Gunn, 1952), where $Z_e = 200R^{1.6}$. The formula derived by direct comparison of

Ze and R in Nagaoka was used for Ze-R relationships for snow ($Z_e = 50.12R^{1.67}$), and graupel ($Z_e = 100R^{1.67}$). A region with large precipitation amounts extended to the west of MP2. Another area of large accumulated precipitation amounts was noted 30–40 km to the west-southwest of MP2. The snowfall amount varied significantly when different Ze-R relationships were used.

Figure 8 shows the distribution of accumulated precipitation during the study period using the tipping-bucket gauge measurement of the AMeDAS, without correction of the wind-induced undercatch. The Ze-R relationship for graupel was closest to the value of the gauge measurement.

Figure 9 shows the scatter diagram of 5-minute CMF at the SIRC site during the study period. Precipitation types were classified using the method described in Section 3. The CMF points classified as graupel, snow aggregate, S1, and S2 categories, respectively, contributed to 61, 9, 8, and 22% of the precipitation during the study period. The graupel and graupel-like snow types were considered the main contributors at the SIRC. Although periods with temperature above 0°C, with a maximum temperature of 0.3°C, were recorded, sleet and rain did not affect the particle classification results, as a plot with notable large fall velocity was not recorded, as seen in Fig. 9.

Similar classifications of data obtained from the Nagaoka University of Technology and Joetsu sites were conducted. Unfortunately, LPM data at the Kashiwazaki, Tochio-Tashiro, and Nishiyama-Yakushi sites were not available during the study period due to human error and insufficient maintenance. The time series of the classification results and precipitation rate are shown in Fig. 10. The predominant precipitation type varied from site to site. However, the predominant type belonged to

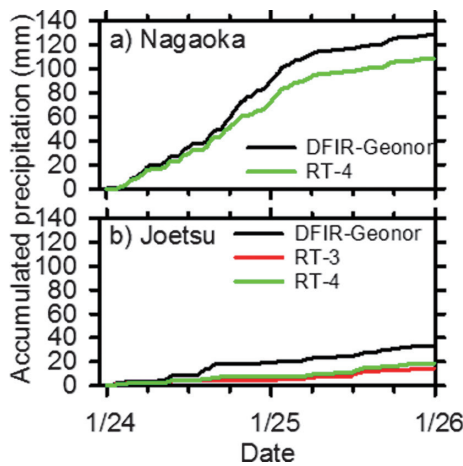


Fig. 6. Time series of accumulated precipitation measured by Geonor, RT-3, and RT-4 at (a) the SIRC, and (b) Joetsu sites from 00:00 JST on January 24, 2016, to 00:00 JST on January 26, 2016. DFIR-Geonor indicates a Geonor gauge installed in the DFIR.

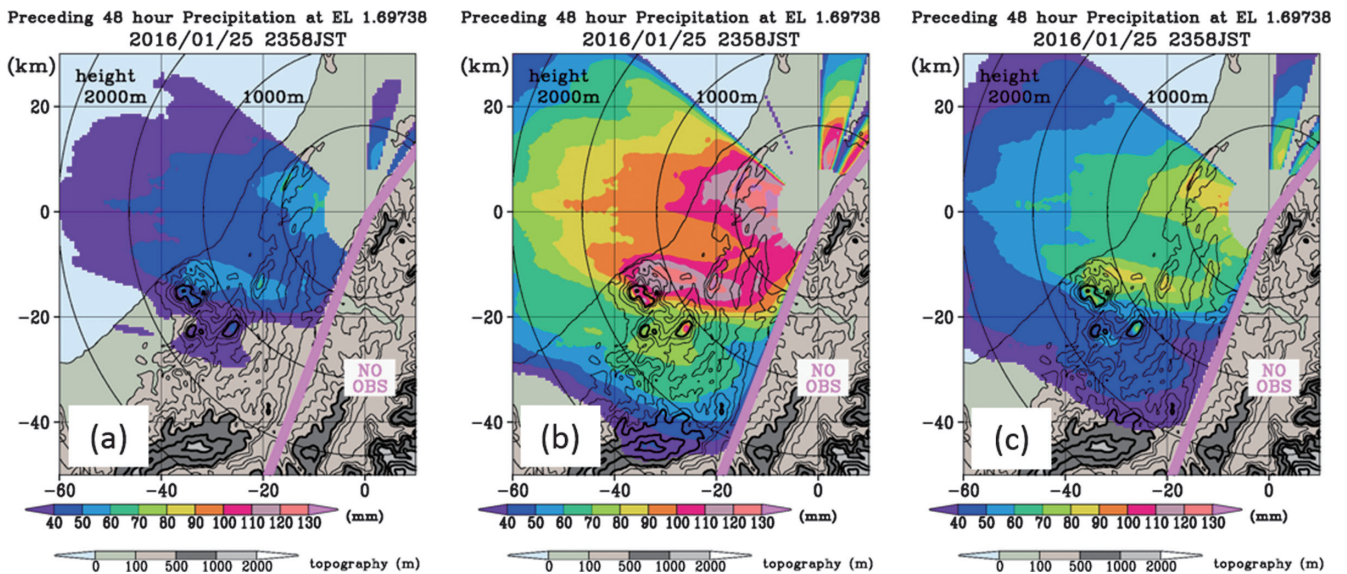


Fig. 7. Distribution of accumulated precipitation over the study period (from January 24 and 25, 2016), estimated from reflectivity factor observed by MP2 at an elevation of 1.7 degrees. Estimation using Ze-R relationships for (a) rain, (b) snow, and (c) graupel are shown. The height of the data is presented by a solid circle in 500 m intervals.

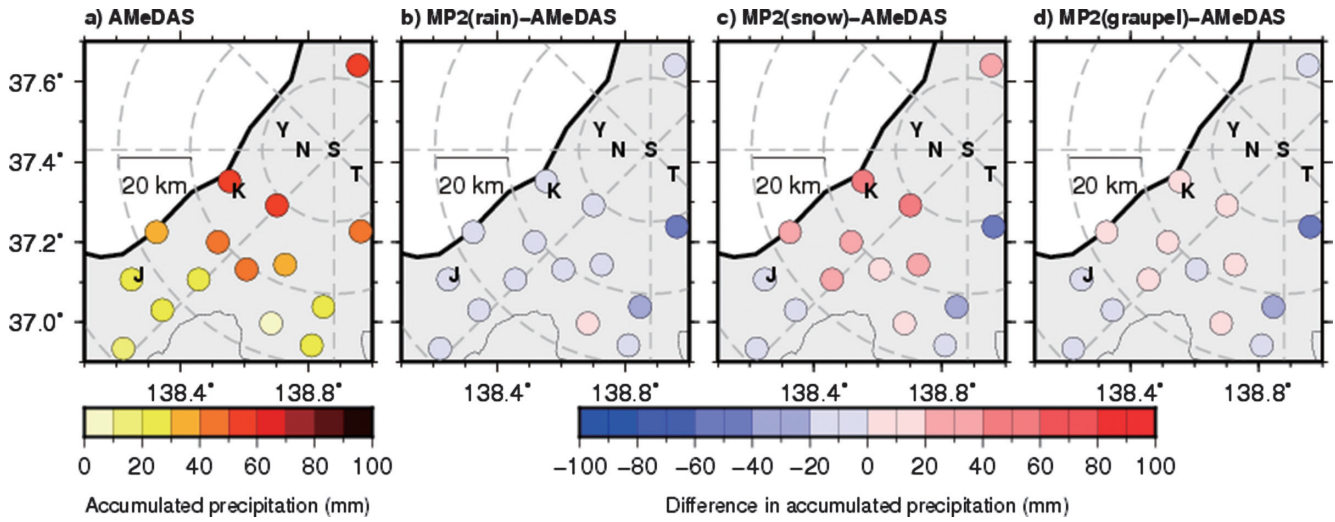


Fig. 8. (a) Distribution of accumulated precipitation from AMeDAS for the study period corresponding to Fig. 7 without undercatch correction. (b-d) Difference in accumulated precipitation between (a) and the estimation from Ze shown in Fig. 7.

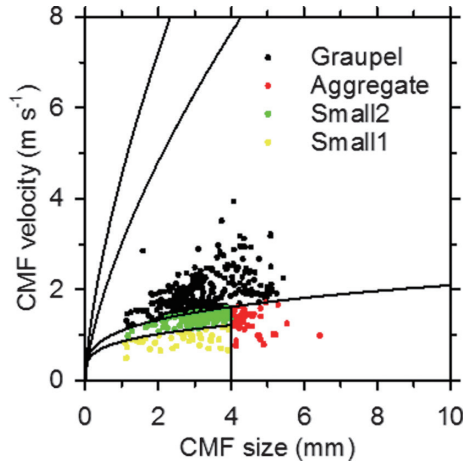


Fig. 9. Scatter diagram of 5-minute CMF, calculated from the LPM observation data at the SIRC site from January 24 to 26, 2016. Solid lines are boundaries of the precipitation particle categories shown in Fig. 4.

one of the graupel categories at all sites during the study period. The radar estimation of the accumulated precipitation using the Ze-R relationship for graupel was closer to the gauge measurement than amounts using other Ze-R relationships (Fig. 8), probably due to longer time duration of graupel precipitation in the observation area. The catch ratio of gauge measurement was not derived for individual solid precipitation particle categories; however, the catch ratio of graupel was expected to be high because of its high fall velocity. It is likely that the gauge measurement was quite close to the correct precipitation amount in this case. Currently, we are trying to improve the existing catch ratio formula and Ze-R relationships of each category of precipitation, both of which are related to the category of precipitation particle. Thus, the distribution of category of precipitation is very important for the improvement of solid precipi-

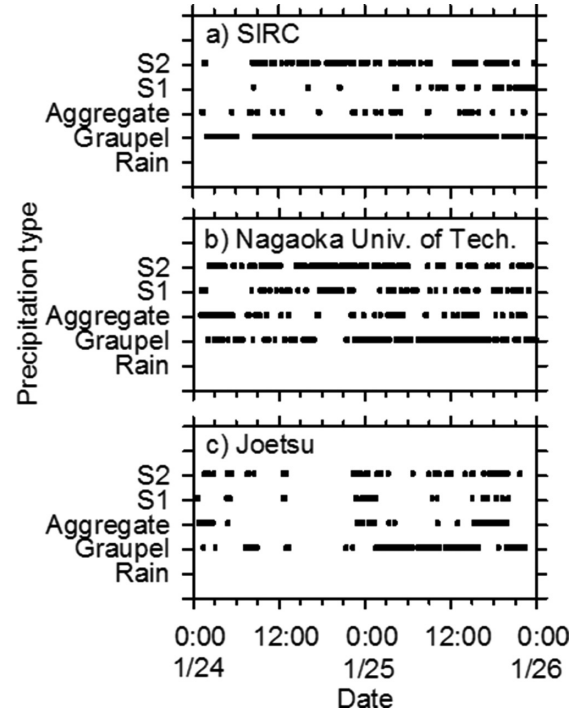


Fig. 10. Time series of precipitation types at (a) SIRC, (b) Nagaoka University of Technology, and (c) Joetsu sites.

tation QPE. Further, we are currently developing a method to estimate the precipitation rate using data of precipitation type distribution from ground observations and radar reflectivity factor distribution.

4.2 Vertical change in precipitation particles at low altitudes

Improved understanding of the change in physical properties (such as size, fall velocity, and Ze-R relationship) of precipitation particles below the beam levels of MP2 can contribute to the development of appropriate Ze-R relationships and accuracy of the QPE.

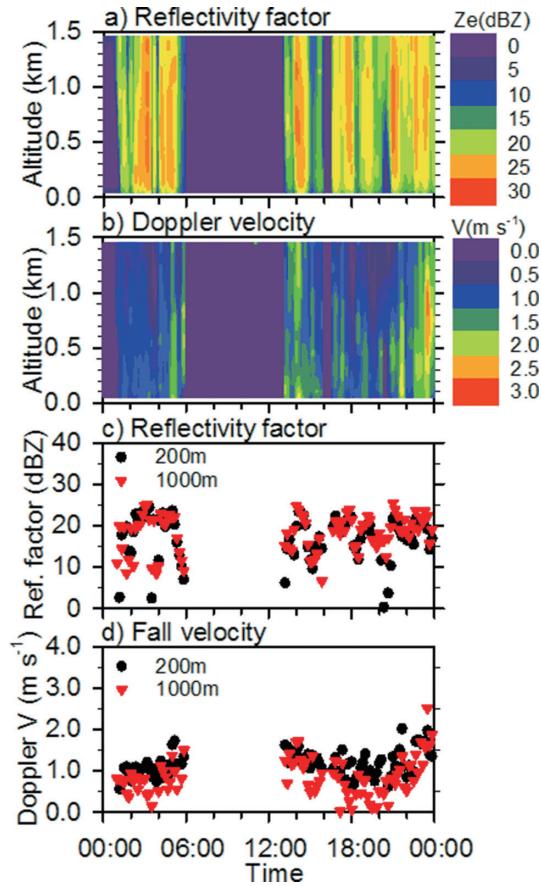


Fig. 11. Time-height cross-section of (a) radar reflectivity factor Z_e (dBZ) and (b) Doppler velocity V (m s^{-1}) over the SIRC site measured by the MRR on January 24, 2016. Time series of (c) Z_e and (d) V at 200 and 1000m altitude.

Figure 11 shows the radar reflectivity factor Z_e (dBZ) and Doppler velocity V (m s^{-1}) over the SIRC site measured by the MRR. Positive V indicates downward motion. Unfortunately, the MRR data for January 25, 2016, was unavailable due to full capacity of the recording device, and from 06:00 JST to 13:00 JST on January 24, 2016, due to snow capping. We noted that heater temperature control in response to snowfall rate and water repellent material coating were necessary to protect against snow capping, which will be implemented in our future research. The Z_e over 200m was almost the same as Z_e over 1000m (Fig. 11c). The V over 200m was larger than V over 1000m (Fig. 11d). However, as this difference included change in the fall velocity, further study is required to analyze the type of meteorological field that affects Doppler velocity, which is needed to distinguish between the fall speed and Doppler velocity. In this case, riming was considered as a factor in the increase in fall velocity as graupel type was dominant from the ground observation data on January 24, 2016 (Fig. 10a).

Figure 12 shows the time series of cloud base height, liquid water path (LWP), and time-height cross-section of temperature estimated from the MWR data at the SIRC site. The neural network technique was used to estimate

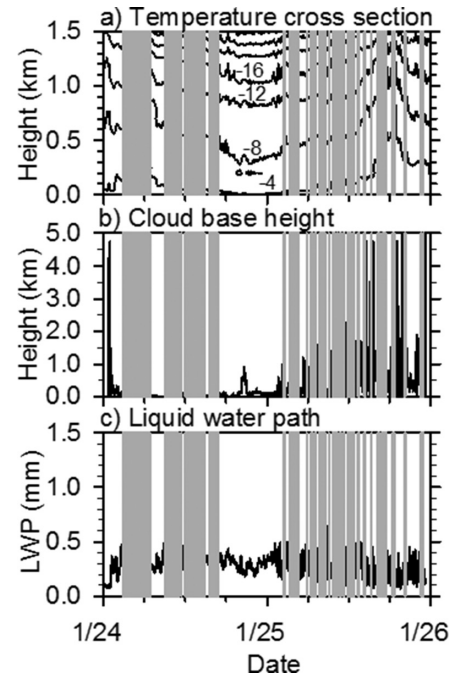


Fig. 12. (a) Time-height cross-section of temperature, and time series of (b) cloud base height, and (c) LWP obtained at the SIRC site from 00:00 JST January 24, 2016 to 00:00 JST January 26, 2016. The contour interval in (a) is 4°C. Measurement data at an elevation angle of 20 degrees and a neural network were used for the estimation of temperature profiles. Shaded areas indicate periods considered to be erroneous.

the vertical profiles of air temperature (Solheim *et al.*, 1998). The shaded areas in Fig. 12 represent the period of time with erroneous data. Based on the webcam monitoring image (not shown here), the error was attributed to a film of water on the MWR's radome as snow capping was detected during that time. Air temperatures over the SIRC site were below 0°C during the study period (Fig. 12a). This indicated that the precipitation particles fell without melting. The cloud base height was less than 500m on most of January 24, 2016, and subsequently increased on January 25, 2016 (Fig. 12b). Sublimation under the cloud base was potentially larger on January 25 than on January 24. Relatively constant profiles and slight decrease in the height of Z_e measured by MRR at levels less than 500m were observed on January 24 and 25, respectively (Fig. 11a), which was consistent with the difference in cloud base height characteristics between the two days (Fig. 12b). LWP values ranging from 0.2 to 0.4 mm (Fig. 12c) and temperature below 0°C indicated the presence of super-cooled droplets over the SIRC site. The obtained values were similar to other values observed in literature (see Table 4).

Size and fall velocity of the precipitation particles measured by optical disdrometers, such as LPM, reflect cloud microphysical processes affecting the precipitation particles. Data obtained using the MRR, MWR, and disdrometers can be used to determine microphysical

Table 4. Measured values of LWP in snow clouds reported in literature.

Site	Observation date	Snow cloud type	LWP range (mm)	References
Akita, Japan	1991 Dec.	Convective snow clouds	<2.0 (mostly <0.5)	Mizuno 2005
Niigata, Japan	1994 Nov. to 1995 Mar.	Orographic snow clouds	<2.0 (mostly <0.2)	Murakami <i>et al.</i> 2001
Toronto, Ontario, Canada	2006 Feb.	Lake-effect snowstorm	<0.9 (mostly <0.4)	Campos <i>et al.</i> 2014
Boulder, Colorado, USA	2008 Feb.	Upslope snowstorm	<1.2 (mostly <0.8)	Campos <i>et al.</i> 2014

change in the falling precipitation particles, which include riming, aggregation, melting, sublimation, and evaporation. Additionally, it can be used to assess the vertical change in precipitation rate between the elevated scanning plane of a weather radar and ground. The analysis of combined data and development of an appropriate algorithm to evaluate the vertical change of precipitation particles are currently being investigated.

5. Summary

We constructed an improved snowfall monitoring system, CSMS, comprised of an X-band weather radar and six ground observation sites to estimate solid precipitation distribution and type with high accuracy. A QPE algorithm using the precipitation type data from ground observations and radar reflectivity factor distribution was developed for this system. At three of the ground observation sites, the vertical Ze and Doppler velocity profiles were measured using MRRs. The vertical profiles of the thermodynamic environment were measured using MWRs.

Preliminary analysis of the snowfall on January 24 and 25, 2016, in central Niigata Prefecture using the CSMS demonstrated that the CSMS successfully generated precipitation rate distributions and precipitation types at the ground observation sites even under heavy snowfall. The distribution of accumulated precipitation over two days (January 24 and 25, 2016), estimated using the MP2 reflectivity factor varied notably when different Ze-R relationships were applied. Currently, a QPE method that accounts for observed precipitation types is under development to eliminate this uncertainty.

The preliminary analysis also showed that the data provided by the CSMS (such as vertical profiles of Ze, Doppler velocity, temperature, cloud base height, LWP, and size and fall velocity of precipitation particles on the ground) were useful for the analysis of change in the precipitation particles, such as riming, aggregation, melting, sublimation, and evaporation. An improved understanding of the vertical change in precipitation particle characteristics will contribute to more accurate QPE for solid precipitation because it acknowledges the differences in precipitation rates between elevated conical planes of scanning radars and the ground. The CSMS offers promising potential for more accurate QPE of solid precipitation, although further quality checks and analysis methods are needed.

Acknowledgments

This research was supported by a management expenses grant for the National Research Institute for Earth Science and Disaster Resilience.

References

- Araki, K. and Murakami, M. (2015): Numerical simulation of heavy snowfall and the potential role of ice nuclei in cloud formation and precipitation development. *CAS/JSC WGNE Research Activities in Atmospheric and Oceanic Modelling*, **45**, 4.03–4.04.
- Atlas, D. and Ulbrich, C. W. (1977): Path- and area-integrated rainfall measurement by microwave attenuation in the 1–3 cm band. *J. Appl. Meteorol.*, **16**, 1322–1331, doi:10.1175/1520-0450(1977)016<1322:paairm>2.0.co;2.
- Bakkehoi, S., Øien, K. and Førland, E. J. (1985): An automatic precipitation gauge based on vibrating-wire strain gauges. *Nord. Hydrol.*, **16**, 193–202, doi:10.2166/nh.1985.0015.
- Bloemink, H. I. and Lanzinger, E. (2005): Precipitation type from the Thies disdrometer. *WMO Technical Conference on Meteorological and Environmental Instruments and Methods of Observation (TECO-2005) Bucharest, Romania*, 4–7 May 2005, 3 (11).
- Campos, E. F., Ware, P., Joe, P. and Hudak, D. (2014): Monitoring water phase dynamics in winter clouds. *Atmos. Res.*, **147**, 86–100, doi:10.1016/j.atmosres.2014.03.008.
- Doviak, R. J. and Zrnic, D. S. (1993): *Doppler radar and weather observations*, second edition. Academic. Press, San Diego, 562 pp.
- Fabry, F. (2015): *Radar meteorology principles and practice*, Cambridge Univ. Press, Cambridge, 256 pp.
- Fujiyoshi, Y., Endoh, T., Yamada, T., Tsuboki, K., Tachibana, Y. and Wakahama, G. (1990): Determination of a Z-R relationship for snowfall using a radar and sensitive snow gauges. *J. Appl. Meteorol.*, **29**, 147–152, doi:10.1175/1520-0450(1990)029<0147:doarfs>2.0.co;2.
- Goodison, B., Louie, P. Y. T. and Yang, D. (1998): *WMO solid precipitation measurement intercomparison final report*. WMO/TD-No. 872, IOM No. 67, World Meteorological Organization, 212 pp.
- Honda, M., Yamazaki, A., Kuwano-Yoshida, A., Kimura, Y. and Iwamoto, K. (2016): Synoptic conditions causing an extreme snowfall event in the Kanto-Koshin district of Japan on 14–15 February 2014. *SOLA*, **11**, 259–264, doi:10.2151/sola.2016-051.
- Ishizaka, M., Motoyoshi, H., Nakai, S., Shiina, T., Kumakura, T. and Muramoto, K. (2013): A new method for identifying the main type of solid hydrometeors contributing to snowfall from measured size-fall speed relationship. *J. Meteorol. Soc. Jpn.*, **91**, 747–762, doi:10.2151/jmsj.2013-602.
- Ishizaka, M., Motoyoshi, H., Nakai, S., Shiina, T., Kumakura, T. and Muramoto, K. (2016): Relationships between snowfall density and solid hydrometeors, based on measured size and fall speed, for snowpack modeling applications. *Cryosphere*, **10**, 2831–2845, doi:10.5194/tc-10-2831-2016.
- Kruger, A. and Krajewski, W. F. (2002): Two-dimensional video disdrometer: A description. *J. Atmos. Oceanic Technol.*, **19**,

- 602-617, doi:10.1175/1520-0426(2002)019<0602:tdvdad>2.0.co;2.
- Locatelli, J. D. and Fobbs, P. V. (1974): Fall speeds and mass of solid precipitation particles. *J. Geophys. Res.*, **79**, 2185-2197, doi:10.1029/jc079i015p02185.
- Maahn, M. and Kollias, P. (2012): Improved micro rain radar snow measurements using Doppler spectra post-processing. *Atmos. Meas. Tech.*, **5**, 2661-2673, doi:10.5194/amt-5-2661-2012.
- Maeda, H. (2007): Damages caused due to heavy snowfall in Hokuriku district in 2006 (in Japanese with English abstract). *J. Jpn. Soc. Snow and Ice (Seppyo)*, **69**, 3-8.
- Marshall, J. S. and Gunn, K. L. S. (1952): Measurement of snow parameters by radar. *J. Meteor.*, **9**, 322-327.
- Marshall, J. S., Hitschfeld, W. and Gunn, K. L. S. (1955): Advances in radar weather. *Adv. Geophys.*, **2**, 1-56, doi:10.1016/s0065-2687(08)60310-6.
- Mizuno, H. (2005): Study of precipitation mechanisms in snow clouds over the Sea of Japan and feasibility of their modification by seeding. *Technical Reports of the Meteorological Research Institute*, **38**, 109-113.
- Murakami, M., Hoshimoto, M., Orikasa, N., Yamada, Y., Mizuno, H., Tokuno, M., Soeda, K., Kajikawa, M., Ikeda, A. and Itsui, M. (2001): Occurrence frequency of snow clouds with high seedabilities over the Echigo Mountains - Statistical evaluation of their appearance frequency with GMS IR channel data and ground-based microwave radiometer data- (in Japanese with English summary). *Tenki*, **48**, 547-559.
- Nakai, S. and Yamaguchi, S. (2012): Snowfall characteristics and the occurrence of related disasters during the heavy snowfall in 2010/2011 winter. -Overview in whole Japan and the concentrated heavy snowfall in Totori- (in Japanese with English summary). *Natural Disaster Research Report of the National Research Institute for Earth Science and Disaster*, **47**, 1-16.
- Rasmussen, R., Dixon, M., Vasiloff, S., Hage, F., Knight, S., Vivekanandan J. and Xu, M. (2003): Snow nowcasting using a real-time correlation of radar reflectivity with snow gauge accumulation. *J. Appl. Meteorol.*, **42**, 20-36, doi:10.1175/1520-0450(2003)042<0020:snuart>2.0.co;2.
- Rasmussen, R., Baker, B., Kochendorfer, J., Meyers, T., Landolt, S., Fischer, A. P., Black, J., Thériault, J. M., Kucera, P., Gochis, D., Smith, C., Nitu, R., Hall, M., Ikeda, K. and Gutmann, E. (2012): How well are we measuring snow: The NOAA/FAA/NCAR winter precipitation test bed. *Bull. Am. Meteorol. Soc.*, **93**, 811-829, doi:10.1175/bams-d-11-00052.1.
- Sato, A. (2006): Heavy snowfall disaster in the winter of 2005-2006 (in Japanese with English summary). *J. Japan Society for Natural Disaster Science*, **25-1**, 71-81.
- Sato, A. (2012): An outline of snow disasters during the winter of 2010/2011 (in Japanese with English summary). *Natural Disaster Research Report of the National Research Institute for Earth Science and Disaster*, **47**, 57-62.
- Solheim, F., Godwin, J., Westwater, E., Han, Y., Keilm, S., Marsh, K. and Ware, R. (1998): Radiometric profiling of temperature, water vapor, and cloud liquid water using various inversion methods. *Radio Sci.*, **33**, 393-404, doi:10.1029/97rs03656.
- Tamura, M. (1993): An automatic system for controlling snow on roofs. *Ann. Glaciol.*, **18**, 113-116, doi:10.1017/s0260305500011356.
- Wakimoto, R. M. and Srivastava, R. C. (2003): *Radar and atmospheric science: A collection of essays in honor of David Atlas Meteorological Monographs*, **52**, American Meteorological Society, Boston, 270 pp.
- Yamazaki, A., Honda, M. and Kuwano-Yoshida, A. (2015): Heavy snowfall in Kanto and on the Pacific Ocean side of northern Japan associated with western Pacific blocking. *SOLA*, **11**, 59-64, doi:10.2151/sola.2015-013.
- Yokoyama, K., Ohno, H., Kominami, Y., Inoue, S. and Kawakata, T. (2003): Performance of Japanese precipitation gauges in winter (in Japanese with English abstract). *J. Jpn. Soc. Snow and Ice (Seppyo)*, **65**, 303-316.
- Zhang, G. (2016): *Weather radar polarimetry*, CRC Press, Boca Raton, 304 pp.